Valorization of coconut peat to develop a novel shape-stabilized phase change material for thermal energy storage

Pin Jin Ong [a], Goh Si Hui Angela [a], Yihao Leow [a], Suxi Wang [a], Pei Wang [a], Zibiao Li [a,b,d], Xuesong Yin [a], Beng Hoon Tan [a], Warintorn Thitsartarn [a], Jianwei Xu [a,b,c], Xian Jun Loh [a,b,d], Dan Kai [a,b,e*], Qiang Zhu [a,b,e*]

a. *Institute of Materials Research and Engineering (IMRE), Agency for Science, Technology and Research (A*STAR), 2 Fusionopolis Way, Innovis #08-03 Singapore 138634, Republic of Singapore*

b. *Institute of Sustainability for Chemicals, Energy and Environment (ISCE^2), Agency for Science, Technology and Research (A*STAR), 1 Pesek Road, Jurong Island, Singapore 627833, Republic of Singapore*

c. *Department of Chemistry, National University of Singapore, 3 Science Drive 3, Singapore 117543, Republic of Singapore*

d. *Department of Material Science and Engineering, National University of Singapore, 9 Engineering Drive 1, #03-09 EA, Singapore 117575, Republic of Singapore*

e. *School of Chemistry, Chemical Engineering and Biotechnology, Nanyang Technological University, 21 Nanyang Link, Singapore 637371, Republic of Singapore*

**Corresponding authors: kaid@imre.a-star.edu.sg;zhuq@imre.a-star.edu.sg*

Abstract

Coconut peat (CP) is a product derived from coconut husks and it has been recognized as a valuable resource for the removal of heavy metals, as an oil-sorbent material, and for agricultural purposes. However, large quantities of coconut husks are still discarded yearly, leading to environmental pollution. In this study, a series of CP/polyethylene glycol (CP/PEG) composites were prepared as novel shape-stabilized phase change materials (SSPCMs) by vacuum impregnation to demonstrate a potential new application of CP in the area of thermal energy storage. The composites were investigated by thermogravimetric (TG) analysis, differential scanning calorimeter (DSC), scanning electron microscopy, attenuated total reflection-Fourier transform infrared spectrometer, leakage test, and thermal cycling testing. The results revealed that the CP/PEG composites exhibit minimal leakage of PEG while the composite with a CP/PEG mass ratio of 3:7 has a high latent heat storage of 108.5 J/g and relative enthalpy efficiency of 91.7%. Meanwhile, TG results indicated that it has good thermal stability up to 150 ℃ and the thermal cycling test showed that it has excellent thermal reliability even after 100 thermal cycles. The heat harvesting and releasing performance of the sample was evaluated as well to understand its thermoregulation capability. Therefore, the obtained CP/PEG composite demonstrates that it can potentially be utilized for thermal storage applications such as in wallboard or building materials for passive cooling, thus fostering a cleaner process by realizing energy savings.

Keywords: Polyethylene glycol, coconut peat, shape-stabilized phase change materials, thermal energy storage, waste recycling

1. Introduction

In recent decades, the rise in global energy consumption and the surge in emissions of greenhouse gases due to rapid urbanization has prompted not only the development of new energy conversion and storage methods (Deborah, et al., 2015; Lee, et al., 2023; Nabavi-Pelesaraei, et al., 2021; Panepinto and Genon, 2012) but also the use of life cycle assessment to assess the impact of these technologies (Hamidinasab, et al., 2023; Hosseinzadeh-Bandbafha, et al., 2017; Nabavi-Pelesaraei, et al., 2023). In this regard, phase change materials (PCMs) have been recognized as efficient thermal energy storage (TES) materials and therefore have been gaining wide attention in recent years. PCMs have high storage density, excellent energy storage-releasing capability at a nearly constant temperature, and good chemical stability. Therefore, PCMs have been broadly applied in many fields, such as solar energy (Wu, et al., 2023; Yang, et al., 2023), buildings (Ong, et al., 2023b; Png, et al., 2022), thermoelectric (Tang, et al., 2020; Yong, et al., 2020; Zhu, et al., 2020), textiles (Lu, et al., 2019; Zhang, et al., 2022), and electronics (Abdulmunem, et al., 2023a; Liao, et al., 2022; Zhu, et al., 2023b).

Based on the type of phase transition, PCMs can be generally divided into two major categories: solid-solid PCMs and solid-liquid PCMs. Solid-solid PCMs do not generate any liquid or gas during phase transition and hence do not require a container to accommodate them. With regard to solid-solid PCM systems, various metal alloys, and processes have been investigated (Kuang, et al., 2018; Qi, et al., 2023; Wang, et al., 2022; Xin, et al., 2022). However, they have small latent heat capacities and supercooling issues, limiting their applications (Yang, et al., 2022a; Zhang, et al., 2023b; Zhao, et al., 2019; Zhu, et al., 2023a). On the other hand, solid-liquid PCMs have been researched and applied extensively for TES systems as they have high latent heat capacities, little or no volume change during phase transition, and good chemical and thermal stabilities (Ong, et al., 2023a; Zare, et al., 2022). Nevertheless, the leakage issue during phase transition prevents their direct usage in applications (Lee, et al., 2022; Soo, et al., 2023). To address this issue, shape-stabilized (or form-stable) PCMs (SSPCMs) can be developed to encapsulate the PCMs in an organic or inorganic matrix using supporting materials such as carbon nanostructures (Göksu, et al., 2022; Huang, et al., 2022b; Liu, et al., 2023), mesoporous silica (Matei, et al., 2019; Mitran, et al., 2020), expanded graphite (Nguyen, et al., 2023; Rathore and kumar Shukla, 2021), expanded vermiculite (Zhang, et al., 2017), and other inorganic structures (Huang, et al., 2022a; Yang, et al., 2022b; Zhang, et al., 2023a).

Poly(ethylene glycol) (PEG), a typical organic PCM, has outstanding properties such as non-toxicity, good thermal stability, relatively high latent heat, and has a variety of molecular weights and therefore has been widely investigated for SSPCMs (Soo, et al., 2022; Sun, et al., 2018). PEG-based SSPCMs can be prepared by embedding PEG into supporting materials with a porous structure, such as graphene oxide (GO) (Ge, et al., 2020; Yang, et al., 2020), diatomite (Ren, et al., 2022), and epoxy resin (Wu, et al., 2018). PEG/mesoporous activated carbon (AC) SSPCMs were prepared using different molecular

weights of PEG via direct blending and impregnation (Feng, et al., 2011). Lower phase transition temperatures and enthalpies were observed as the molecular weight of PEG decreased while the crystallinity of PEG in the PCMs decreased with an increase in AC content. PEG/SiO_2 SSPCM was successfully developed (Li, et al., 2020), whereby the composite has a high phase change enthalpy of 164.9 J/g with a PEG mass fraction of 97%. On the other hand, PEG/GO SSPCMs were synthesized with the assistance of a microwave (Xiong, et al., 2015). The maximum PEG content in the composite reached 96 wt%, leading to a high heat storage capacity of 174.5 J/g. In another case, hydroxylated carbon nanotubes were added to PEG to improve the thermal conductivity and shape stability (Yang, et al., 2022c). The composites have a phase change enthalpy of 119.9 ~ 127.9 J/g and an improved thermal conductivity of 2.2 times that of PEG. Most of the aforementioned studies are conducted for applications in TES but the supporting materials used such as GO, SiO_2 and diatomite are either costly or have low porosity, thus affecting their applicability.

Research on upcycling of waste materials has gained popularity in recent years (Cao, et al., 2022; Jiang, et al., 2023; Muiruri, et al., 2023; Pourebrahimi, 2022) and this is due to heightened environmental concerns, technological advancements, and a growing emphasis on circular economy principles. For example, recycled waste paper was used as a thermal insulation material in conjunction with paraffin wax for building cooling applications (Abdulmunem, et al., 2023b). The results indicated that the indoor room temperature was reduced by 9.6% while an optimal waste paper ratio of 75% reduced the electricity cost and cooling load by 16.3% and 19%, respectively. In another interesting investigation, waste chicken feathers were mixed with paraffin wax and this bio-composite material was integrated into polyvinyl chloride panels as building inner envelopes (Abdulmunem, et al., 2022). According to the results, the panels have a flexural strength of 0.55 MPa and maximum tensile strength of 3.75 MPa. A reduction in noise levels and electricity costs by 9% and 22.5%, respectively were noted as well. On the other hand, high-density polyethylene plastic wastes were converted into hierarchical porous carbon materials and high-purity methane via autogenic pressure hydrolysis and KOH activation for high-performance supercapacitors (Zhou, et al., 2023). The porous carbon materials which can be used as electrode materials, have high specific surface area (2785-2913 m^2/g), high specific capacitance (301 F/g at 1 A/g), and a rate performance of 89.1% at 20 A/g. Coconut peat (CP) is a product derived from coconut husks and this fruit is naturally abundant in many Asian countries such as the Philippines, Thailand, Malaysia, and China (Keerthika, et al., 2016). The main constituent of CP is lignocellulose, which comprises lignin (~49%), cellulose (~43%), and hemicellulose (~8%) (Thakur, et al., 2015). Large quantities of coconut husks are discarded as biomass waste yearly due to their low economic value and this leads to environmental pollution. However, CP does offer many underutilized benefits such as high availability, biodegradability, and low cost. In view of this, researchers have explored different ways of utilizing this material and they are found to have the potential for applications as an oil-sorbent material (Phat, et al., 2022; Verasoundarapandian, et al., 2021; Yang, et al., 2017), the

removal of heavy metals (Saeed, et al., 2021; Saman, et al., 2016; Sireesha and Sreedhar, 2023) and for agricultural purposes as well. Nevertheless, the studies of CP for other applications have not been extensively carried out.

To our best knowledge, the application of CP has not been implemented in the realm of TES previously. Therefore, the objective of this work is to investigate and demonstrate a new and alternative approach to utilizing CP besides the aforementioned instances. In this study, we have opened up yet another possibility of valorizing CP by utilizing it as a supporting material for the preparation of SSPCMs for the first time. A series of SS PEG-based PCMs were prepared via vacuum impregnation and the influence of different CP contents on the composites was investigated by characterizations of their structures, morphologies, and thermal properties. This study has demonstrated an alternative method to broaden the potential applications of CP in the area of TES such as passive cooling in building materials through a facile preparation of SSPCMs. By utilizing waste materials and potentially reducing energy consumption, this work confers the benefits of achieving sustainability.

2. Materials and methods

2.1. Materials

Poly(ethylene glycol) (PEG, average M_n = 2050 g/mol) was purchased from Sigma Aldrich. Raw coconut peat was purchased from Nextevo^{TM}. It was washed with deionized (DI) water three times to remove any physical impurities and dried overnight in the oven at 100 ℃ before use.

2.2. Preparation of CP/PEG composite shape-stabilized PCMs

The CP/PEG composites with different mass ratios of CP/PEG (6:4, 5:5, 4:6, 3:7, and 2:8) were fabricated via the vacuum impregnation method. For example, the typical preparation process for a mass ratio of 6:4 is as follows: 0.4g of PEG was dissolved in 25 mL of DI water and 0.6g of CP was added to the mixture. The sample is sonicated for 1.5 h and thereafter placed in a vacuum oven at 60 ℃ for 12 h under 0.02 MPa. Finally, the CP/PEG composite was fabricated and identified as CP6_PEG4. The CP/PEG composites with different mass ratios are shown in Table 1.

Table 1. Mass fractions of CP and PEG in CP/PEG composites.

Sample	Mass ratio of CP/PEG	Mass of CP (g)	Mass of PEG (g)
CP6_PEG4	6:4	0.6	0.4
CP5_PEG5	5:5	0.5	0.5
CP4_PEG6	4:6	0.4	0.6

CP3_PEG7	3:7	0.3	0.7
CP2_PEG8	2:8	0.2	0.8

2.3. Characterization

2.3.1. Structural and morphological analysis

The characteristic functional groups of PEG and the CP/PEG composites were analyzed using a Vertex 80 attenuated total reflection-Fourier transform infrared spectrometer (ATR-FTIR) (Bruker). The analyses were conducted at room temperature, with a total of 64 scans and a spectrum resolution of 4 cm^{-1} over the frequency range of 4000 to 400 cm^{-1}. The morphological study of PEG and the CP/PEG composites was carried out using a scanning electron microscope (SEM) (JEOL JSM6700F). The samples were coated with a thin layer of gold using sputter coating and the micrographs were taken with 10 µA emission current and 5 kV acceleration voltage in a high vacuum mode.

2.3.2. Thermal analysis

The thermal stability of the CP/PEG composites was evaluated on the thermogravimetric analyzer (Q500, TA Instruments, USA). Each sample was placed in an alumina crucible and heated at a rate of 20 °C/min from room temperature to 900 °C under a nitrogen atmosphere. The phase change temperature and thermal enthalpy of the CP/PEG composites were evaluated using a differential scanning calorimeter (DSC) (Q100, TA instruments, USA). Each sample was encapsulated in an aluminum hermetic pan, heated, and cooled at a rate of 10 °C/min in a nitrogen atmosphere in the range of -10 °C to 80 °C. To assess the thermal reliability of the composites, 100 consecutive melt/freeze cycles were conducted using the aforementioned DSC equipment. For each cycle, the samples were heated from -10 °C to 80 °C at a rate of 20 °C/min and held for 1 min, then cooled from 80 °C to -10 °C at the same rate and held for 1 min.

2.3.3. Form stability and leakage test

The CP/PEG composites were subjected to a leakage test to determine the form stability. 0.4 g of PEG and each CP/PEG composite were made into a pellet by pressing it at a pressure of 4 tons for 1 min with a manual hydraulic press (Specac). Each pellet has a diameter of 1.3 cm and a thickness of 3 mm and the initial mass (M_0) of each sample was measured. All the samples were each placed on a filter paper in a petri dish and placed in the oven at 75 °C for 8 h. The samples were taken out from the oven and allowed to cool down before measuring the weight (M_n) at intervals of 1 h. Optical images of the samples before and after the leakage test were taken and the leakage rate (L) was calculated as per Equation (1):

$$L = \frac{M_0 - M_n}{M_0} \times 100\% \quad (1)$$

2.3.4. Heat harvesting and releasing performance

1.5 g of CP3_PEG7 was made into a pellet using the same equipment and experimental condition aforementioned and the pellet has a diameter of 2 cm and a thickness of 3 mm. A heating module, measuring 5.5 cm × 5.5 cm served as the heat source, and positioned directly above it was an infrared radiation (IR) camera (FLIR A65) to capture IR images and monitor temperature fluctuations. The heating module was initially raised to and sustained at 100 °C. Subsequently, CP3_PEG7 was positioned on it and permitted to heat until reaching 80 °C. Following this, the module was switched off, enabling the sample to cool down. The experiment was conducted with an ambient temperature of 21 °C.

3. Results and discussion

3.1. Thermogravimetric analysis

The thermogravimetric (TG) and derivative TG (DTG) curves of CP and the CP/PEG composites are shown in Figure 1 whilst the thermal decomposition data are shown in Table 2. For PEG, there is an obvious degradation step in the temperature of 188.1 to 432.5 ℃, which is attributed to the decomposition and evaporation of the organic alcohol compounds. For CP and the CP/PEG composites, two major degradation steps can be seen in the thermograms. The first stage of degradation that occurs between 32.9 to 150.3 ℃ is due to the elimination of adsorbed water molecules on CP. Even though CP has undergone drying prior to use, its hydrophilic nature makes the structurally bound water molecules resistant to complete evaporation during the drying process. This mass loss of 8.4% for CP is consistent with other previously reported work (Hosokawa, et al., 2016; White, et al., 2011), which is within the range of 5-10%. This value decreased as the loading of CP decreased in the composites, reaching a value of 1.4% for CP2_PEG8. The second stage of degradation, which is the main degradation stage, occurs due to the decomposition of hemicellulose, cellulose, and lignin. For CP, it has a peak temperature of 342.6 ℃. As the loading of PEG increased in the composites, understandably there was an increase in the peak temperature from 354.8 to 406.7 ℃, which is approaching the peak temperature of 409.4 ℃ for PEG. Among the three components present in CP, it was reported that lignin has the highest thermal stability, followed by cellulose and hemicellulose (Faulstich de Paiva and Frollini, 2006). Even though lignin started to decompose at a lower temperature (160 to 175 ℃), its decomposition occurred slowly under the whole temperature range up to 900 ℃ (Mittal and Chaudhary, 2019) and the high lignin content in CP led to the relatively high amount of residues of 13.6% at the

end of the analysis. Based on these results, the composites showed thermal stability up to 150 ℃ and hence are suitable for TES applications.

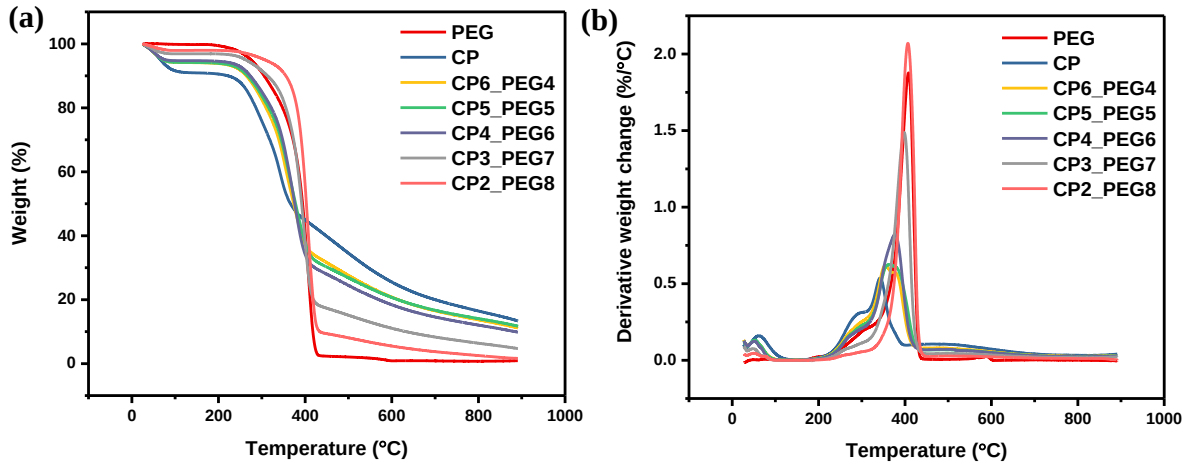

Fig. 1. (a) Thermogravimetry (TG), and (b) Derivative thermogravimetry (DTG) curves of PEG, CP, and CP/PEG composites.

Table 2. TG/DTG decomposition data of PEG and the CP/PEG composites.

Sample	Temperature range (℃)	Peak temperature (℃)	Weight loss (%)	Residual mass (%)
PEG	188.1-432.5	409.4	97.1	1.5
CP	32.9-150.3	61.3	8.4	13.6
	150.3-402.3	342.6	46.3	
CP6_PEG4	33.9-107.3	53.2	4.9	11.7
	145.8-429.7	354.8	60.8	
CP5_PEG5	34.9-103.2	52.2	4.8	11.2
	163.4-443.8	363.9	63.6	
CP4_PEG6	37.3-88.6	51.2	4.0	9.8
	189.5-433.7	377.0	65.5	
CP3_PEG7	38.2-74.6	50.3	2.0	4.7
	191.3-451.1	397.6	79.6	
CP2_PEG8	38.7-70.7	49.5	1.4	1.7
	192.6-456.8	406.7	88.8	

3.2. DSC analysis

The thermal energy storage performance of the CP/PEG composites was evaluated by DSC and the corresponding thermograms, phase change enthalpies, and phase change temperatures are illustrated in Figures 2a-c. In addition, the enthalpy efficiency (λ) and relative enthalpy efficiency (η) of the composites as defined in Equations 2 and 3, are calculated and shown in Figure 2d.

$$\lambda = \frac{\Delta H_{\mathrm{m(SSPCM)}}}{\Delta H_{\mathrm{m(PEG)}}} \times 100\% \tag{2}$$

$$\eta = \frac{\Delta H_{\mathrm{m(SSPCM)}}}{\Delta H_{\mathrm{m(PEG)}} \times w} \times 100\% \tag{3}$$

where $\Delta H_{\mathrm{m(SSPCM)}}$ and $\Delta H_{\mathrm{m(PEG)}}$ represent the melting enthalpy of the SSPCM and pure PEG, respectively, while w denotes the mass fraction of PEG in the SSPCM.

As shown in Figure 2a, the CP/PEG composites exhibit obvious endothermic and exothermic processes similar to PEG while PEG has melting and crystallization temperatures and corresponding enthalpies of 55.2 ℃, 28.3 ℃, 169.1 J/g and 166.4 J/g, respectively (Figures 2b, c). Compared to the melting and crystallization temperature of PEG, the melting temperature of the CP/PEG composites remained relatively similar, but the crystallization temperature shifted downward. This can be attributed to a confined crystallization environment, which restricts the free movement of PEG molecular chains. On the other hand, a gradual reduction in the melting and crystallization enthalpy is observed for the CP/PEG composites containing different amounts of PEG. The thermal enthalpy of PEG originates from the phase transition of crystalline to amorphous state or vice versa. Clearly, the thermal enthalpy is directly associated with the mass fraction of PEG and the theoretical melting enthalpy of CP6_PEG4, CP5_PEG5, CP4_PEG6, CP3_PEG7, and CP2_PEG8 is 67.6, 84.6, 101.5, 118.4, and 135.3 J/g, respectively. However, the melting enthalpy of all of the CP/PEG composites is lower than their corresponding theoretical values, which implies that a small fraction of PEG does not undergo phase transition. This is attributed to the strong intermolecular hydrogen bonding interactions between PEG and CP, resulting in a small fraction of PEG existing in the amorphous state. Additionally, the η of the CP/PEG composites is as high as 95.8%, 91.7%, 90.5%, 88.5%, and 87.9%, which is higher than most of the reported values in the literature (Huang, et al., 2017; Li and Wang, 2019; Liu, et al., 2020; Wu, et al., 2021; Yan, et al., 2021; Yin, et al., 2021). These results indicate that the CP/PEG composites have excellent thermal storage capacity and high relative enthalpy efficiency.

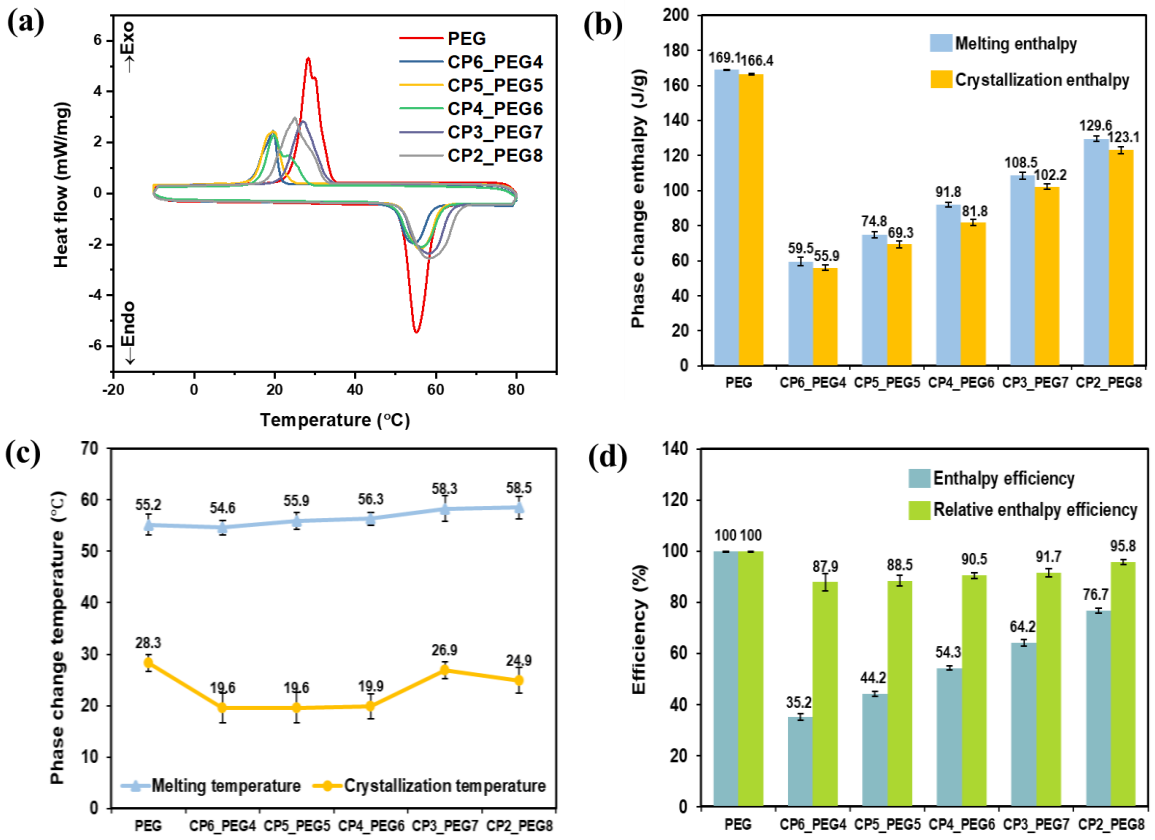

Fig. 2. (a) DSC curves, (b) Phase change enthalpies, (c) Phase change temperatures, and (d) Enthalpy efficiencies of PEG and CP/PEG composites.

3.3. SEM analysis

The morphologies of PEG and the CP/PEG composites are shown in Figure 3. As shown in Figure 3b, CP has a smooth surface with a rod-like structure from the side view while the top view (Figure 3c) revealed that CP has irregular and large hole-like pores, resembling that of a honeycomb structure. On the other hand, the morphology of CP changes significantly after the absorption of PEG (Figures 3d-h). It is observed that CP serves as a supporting material and PEG is adhered to its surface. As the loading of PEG increases, less visible structures of CP are observed, resulting in a rough surface morphology. This implied the efficient absorption of PEG into CP.

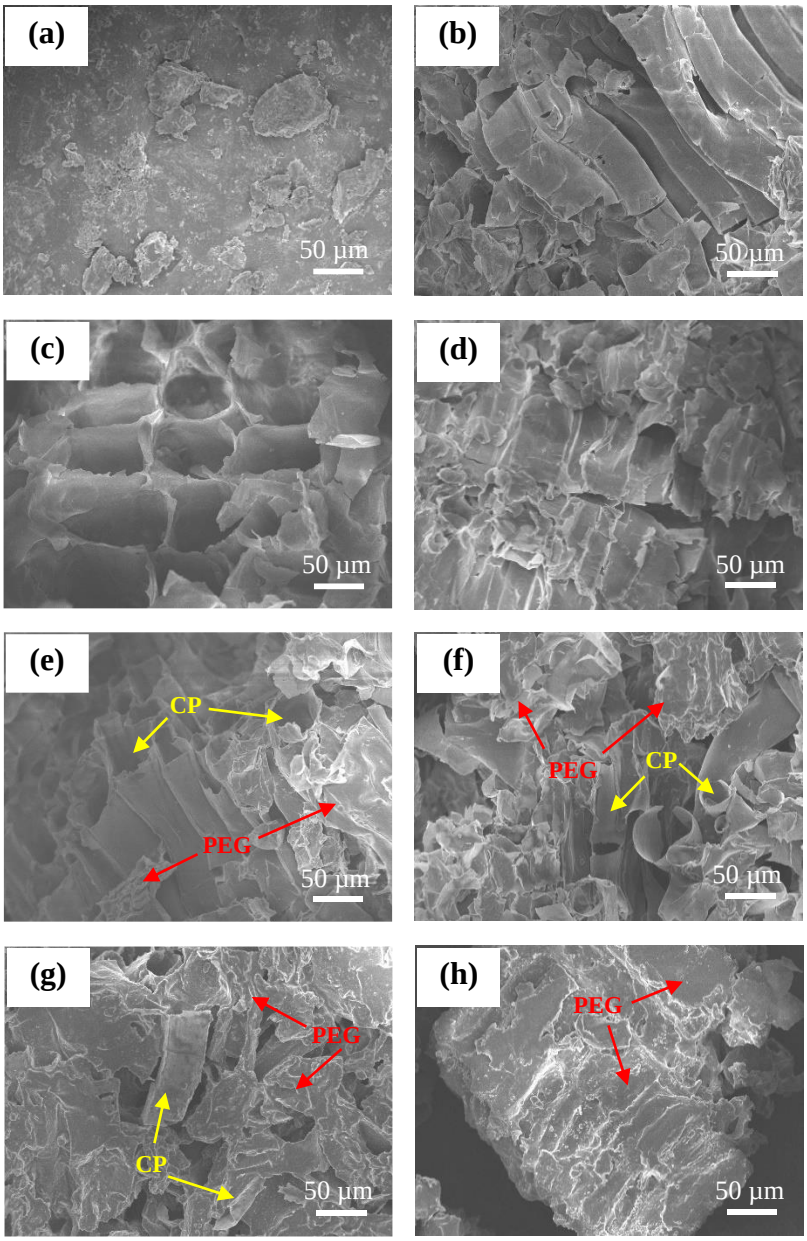

Fig. 3. FE-SEM images of (a) PEG, (b-c) CP, (d) CP6_PEG4, (e) CP5_PEG5, (f) CP4_PEG6, (g) CP3_PEG7, and (h) CP2_PEG8.

3.4. ATR-FTIR analysis

The FTIR spectra of PEG, CP and the CP/PEG composites were examined and are shown in Figure 4. In the spectrum of PEG, the broad adsorption peak at 3402 cm^{-1} is due to the stretching vibrations of the O–H group while the strong characteristic peaks at 2881 cm^{-1} and 1097 cm^{-1} are ascribed to the stretching vibration of C–H and C-O-C, respectively. Meanwhile, the peaks at 1466 cm^{-1} and 1359 cm^{-1} are due to the C-H bending vibrations. As for the CP spectrum, the broad peak at 3398 cm^{-1} is attributed to the O-H stretching of the hydroxyl group while the peak at 2882 cm^{-1} is responsible for the asymmetric and symmetric stretching of C-H groups. The peak at 1636 cm^{-1} is ascribed to the aromatic

C=C stretching in lignin (Liang, et al., 2009) and the peak at 1340 cm^{-1} is assigned to C-H bending vibrations (Wang, et al., 2013). The strong absorption peak at 1099 cm^{-1} is due to C-O stretching in cellulose, hemicellulose, and lignin (Li, et al., 2013). By comparison, it can be seen that as the loading of PEG increases, the intensity of the peaks (C-H and C-O-C stretching) increases as well due to the higher intensity of these peaks of PEG compared to CP. Compared to CP and PEG, no signs of new or a loss of peaks were noted for the CP/PEG composites, which suggests that only physical interactions and no chemical reactions took place during the impregnation process. In addition, a slight shift of the hydroxyl peak is observed for the CP/PEG composites, suggesting that an intermolecular hydrogen bonding interaction has taken place between CP and PEG.

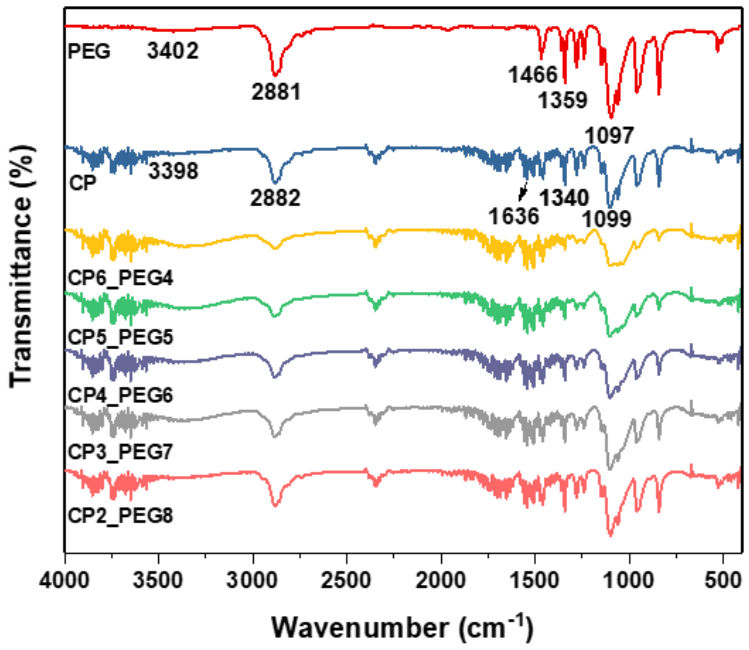

Fig. 4. FTIR spectra of CP, PEG, and CP/PEG composites.

3.5. Leakage test

A series of CP/PEG composites with different mass fractions of PEG were prepared and a leakage test was performed to evaluate the leakage situation and their form stability. Therefore, the leakage test was conducted at 75 °C, which is above the melting point of PEG. Figure 5a shows the optical photographs of PEG and the CP/PEG composites before and after the leakage test while Figure 5b reveals the leakage rate throughout the leakage test at intervals of 1 h. As shown in Figure 5a, the CP/PEG composites have slightly different appearances, corresponding to the different loading of PEG in the composites. It is clear that PEG melted and became a transparent liquid at the end of the leakage test while on the other hand, there were no obvious signs of leakage coming out of the CP/PEG composites and that they demonstrated excellent shape stability. In Figure 5b, the leakage rates after 8 h were 1.14%, 1.35%,

1.60%, 1.99%, and 2.87% for CP6_PEG4, CP5_PEG5, CP4_PEG6, CP3_PEG7, and CP2_PEG8 composites, respectively. In general, the CP/PEG composites exhibited minimal leakage and hence implied that they have good form stability. Nevertheless, the stability and leakage performance is not as good as that of PCMs obtained by chemical means such as chemical grafting. To enhance the interaction between PEG and CP and potentially eliminate the leakage issue, CP could be modified or a chain extender could be covalently bonded to PEG to form PCMs with chemically cross-linked structures. However, the implementation of such processes is more costly and this will hinder its scalability for applications as more chemicals and procedures are involved. Considering the leakage rate and thermal enthalpy of the CP/PEG composites, CP3_PEG7 was selected as the promising candidate for TES applications and hence was subjected to a thermal cycling test to evaluate its thermal reliability (to be discussed in the next section).

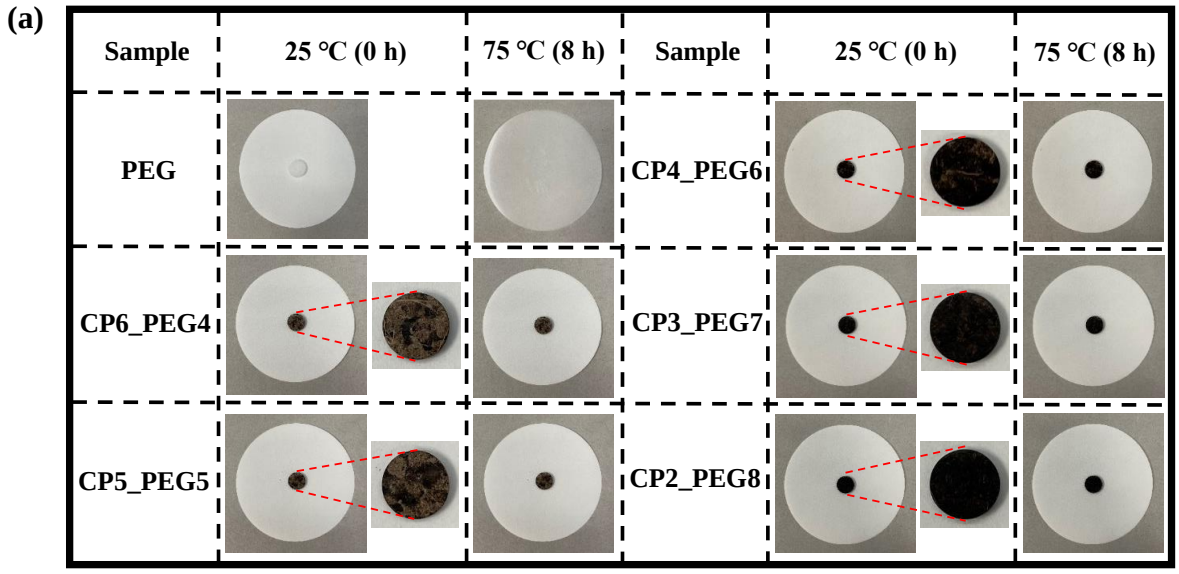

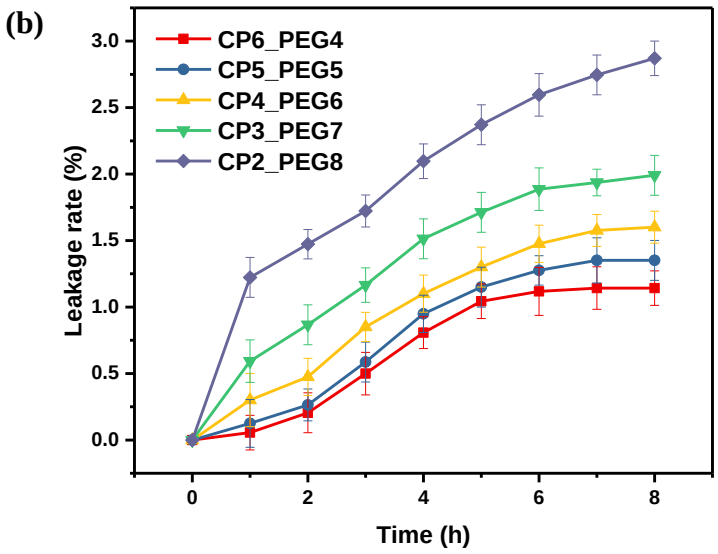

Fig. 5. (a) Leakage test analysis of PEG and CP/PEG composites at 75 °C for 8 h, and (b) Leakage rate of CP/PEG composites.

3.6. Thermal cycling analysis

To assess the suitability of CP3_PEG7 for long-term usage in TES applications, it was subjected to 100 thermal cycles to evaluate its thermal reliability. The DSC thermograms and the analysis results before and after 1, 25, 50, 75, and 100 cycles are shown in Figures 6a-c. Overall, the DSC curves displayed high similarity in terms of shape, with almost identical endothermic peaks. The thermal enthalpies and phase change temperatures are largely uninfluenced by thermal cycling as both of these parameters have minimal dissimilarity as compared to their uncycled values. In addition, to evaluate the chemical stability of the composite after 100 thermal cycles, the FTIR spectrum was examined and compared to its uncycled counterpart (Figure 6d). Both spectra have similar characteristic peaks and no disappearance of any peaks was observed, suggesting that the chemical structure of the composite was unaltered during thermal cycling. The abovementioned results imply the composite is chemically stable, has good thermal reliability, and hence is a promising PCM for TES.

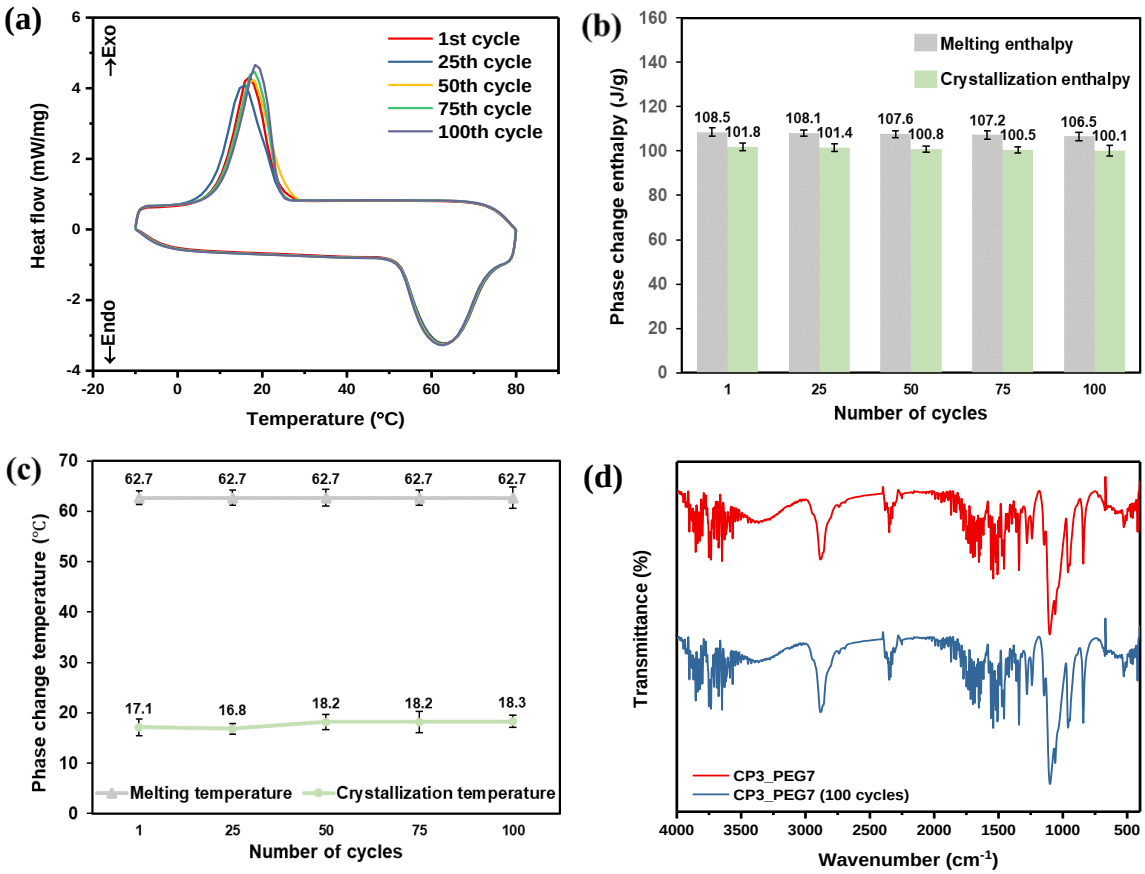

Fig. 6. (a) DSC thermograms, (b) phase change enthalpies, (c) phase change temperatures during 100 thermal cycles, and (d) FTIR spectra of CP3_PEG7 before and after thermal cycling.

3.7. Heat harvesting and releasing performance results

It is essential to understand the thermoregulation capability of the CP/PEG composites and therefore an experimental study was conducted to demonstrate the heat harvesting and releasing performance. The experimental setup and the IR images of CP3_PEG7 with its temperature profile are shown in Figure 7. Figure 7a shows the CP3_PEG7 sample on the heating module, where 'X' on the inset denotes the position at which the temperature logging was recorded via IR imaging. Figure 7b shows that the temperature of CP3_PEG7 increases sharply from the beginning of the experiment up to 75s, where a slight plateau and a change in gradient were observed. This can be attributed to the onset of the solid-solid phase transition in the sample, where the rate of temperature rise is reduced due to the slightly broad melting peak of CP3_PEG7 as shown in Figure 2a. The sample continued to absorb heat up to 359s, which at this point has reached its maximum heat storage capacity, and the temperature continued to rise slowly as it approached the temperature of the heating module. Based on the mass of the sample and its latent heat, it can be determined that 162.8 J of heat energy can be harvested within 359s. At 584s, the module was switched off and the sample started to cool down. At 1095s, several gently sloping plateaus started to appear up to the end of the experiment, and this corresponded to the solid-solid phase change during cooling.

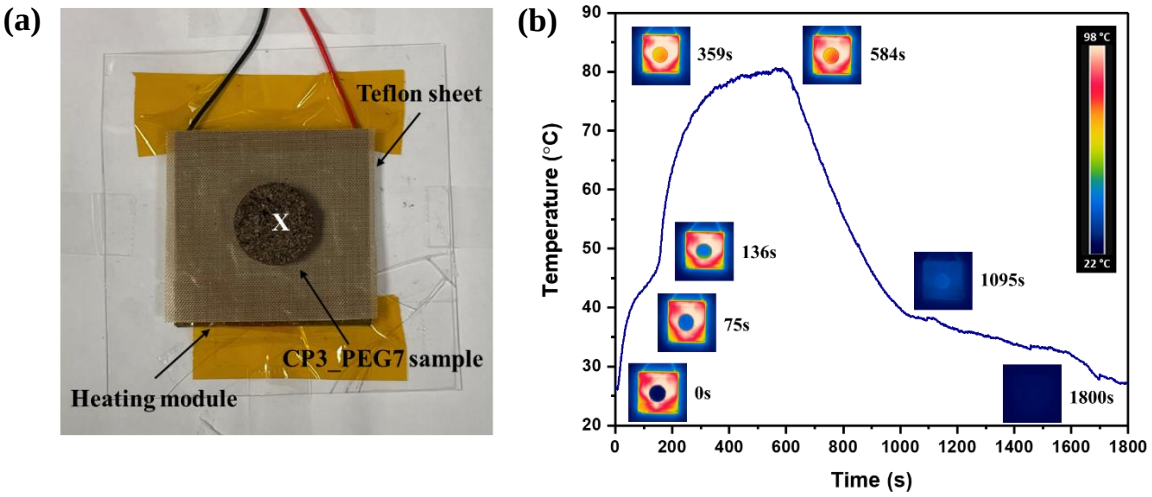

Fig. 7. (a) Experimental setup of the heating module with CP3_PEG7, and (b) IR-imaging of CP3_PEG7 and its temperature profile over time.

4. Conclusion

In summary, the CP/PEG composite SSPCMs have been facilely devised and prepared via a simple direct impregnation method. The composites were prepared via a clean production process as no organic solvents were involved and no waste by-products were produced. The leakage test indicates great shape stability performance of the composites with minimal leakage of PEG while ATR-FTIR analysis results

show that only physical interactions took place between CP and PEG. DSC analysis shows that CP3_PEG7 has a high latent heat storage of 108.5 J/g while the relative enthalpy efficiency is as high as 91.7%. Furthermore, the thermal cycling and TG results demonstrate excellent thermal reliability and good thermal stability of the composite, respectively. An experimental study was conducted as well to evaluate the heat harvesting and releasing performance to understand its thermoregulation capability. In light of our results, we have uncovered yet another possibility of utilizing waste materials such as CP and upcycling them through an innovative combination with PEG to fabricate SSPCMs for TES applications such as in wallboard or building materials for passive cooling. By leveraging the abundance and sustainable nature of CP, the integration of these two components unveils new possibilities for other eco-friendly materials for the development of SSPCMs while promoting cleaner and sustainable production at the same time. Nevertheless, further optimizations such as the addition of nano additives to enhance the thermal conductivity or modifications to CP to improve the leakage performance are required to further enhance the performance characteristics of the SSPCMs.

Abbreviations

AC	Activated carbon
ATR-FTIR	Attenuated total reflection-Fourier transform infrared spectrometer
CP	Coconut peat
DI	Deionized
DSC	Differential scanning calorimeter
DTG	Derivative thermogravimetric
GO	Graphene oxide
IR	Infrared radiation
PCM	Phase change material
PEG	Polyethylene glycol
SEM	Scanning electron microscope
SSPCM	Shape-stabilized phase change material
TES	Thermal energy storage
TG	Thermogravimetric

Declaration of Competing Interest

The authors declare that they have no known competing financial interests or personal relationships that could have appeared to influence the work reported in this paper.

Data availability

Data will be made available on request.

Acknowledgments

This work is supported by the A*STAR Career Development Fund (Grant Number: C210812038).

References

Abdulmunem, A.R., Hamed, H.M., Samin, P.M., Mazali, I.I., Sopian, K., 2023a. Thermal management of lithium-ion batteries using palm fatty acid distillate as a sustainable bio-phase change material. J. Energy Storage 73, 109187. https://doi.org/10.1016/j.est.2023.109187.

Abdulmunem, A.R., Hussein, N.F., Samin, P.M., Sopian, K., Hussien, H.A., Ghazali, H., 2023b. Integration of recycled waste paper with phase change material in building enclosure. J. Energy Storage 64, 107140. https://doi.org/10.1016/j.est.2023.107140.

Abdulmunem, A.R., Samin, P.M., Sopian, K., Hoseinzadeh, S., Al-Jaber, H.A., Garcia, D.A., 2022. Waste chicken feathers integrated with phase change materials as new inner insulation envelope for buildings. J. Energy Storage 56, 106130. https://doi.org/10.1016/j.est.2022.106130.

Cao, J., Sim, Y., Tan, X.Y., Zheng, J., Chien, S.W., Jia, N., Chen, K., Tay, Y.B., Dong, J.F., Yang, L., Ng, H.K., Liu, H., Tan, C.K.I., Xie, G., Zhu, Q., Li, Z., Zhang, G., Hu, L., Zheng, Y., Xu, J., Yan, Q., Loh, X.J., Mathews, N., Wu, J., Suwardi, A., 2022. Upcycling silicon photovoltaic waste into thermoelectrics. Adv. Mater. 34 (19), 2110518. https://doi.org/10.1002/adma.202110518.

Deborah, P., Francesca, V., Giuseppe, G., 2015. Analysis of the environmental impact of a biomass plant for the production of bioenergy. Renew. Sustain. Energy Rev. 51, 634-647. https://doi.org/10.1016/j.rser.2015.06.048.

Faulstich de Paiva, J.M., Frollini, E., 2006. Unmodified and modified surface sisal fibers as reinforcement of phenolic and lignophenolic matrices composites: thermal analyses of fibers and composites. Macromol. Mater. Eng. 291 (4), 405-417. https://doi.org/10.1002/mame.200500334.

Feng, L., Zheng, J., Yang, H., Guo, Y., Li, W., Li, X., 2011. Preparation and characterization of polyethylene glycol/active carbon composites as shape-stabilized phase change materials. Sol. Energy Mater. Sol. Cells 95 (2), 644-650. https://doi.org/10.1016/j.solmat.2010.09.033.

Ge, J., Wang, Y., Wang, H., Mao, H., Li, J., Shi, H., 2020. Thermal properties and shape stabilization of epoxidized methoxy polyethylene glycol composite PCMs tailored by polydopamine-functionalized graphene oxide. Sol. Energy Mater. Sol. Cells 208, 110388. https://doi.org/10.1016/j.solmat.2019.110388.

Göksu, H., Aydınlı, E., Hekimoğlu, G., Sarı, A., Gencel, O., Subaşı, S., Tozluoğlu, A., 2022. Activated carbon nanotube/polyacrylic acid/stearyl alcohol nanocomposites as thermal energy storage effective shape-stabilized phase change materials. Surf. Interfaces 31, 102088. https://doi.org/10.1016/j.surfin.2022.102088.

Hamidinasab, B., Javadikia, H., Hosseini-Fashami, F., Kouchaki-Penchah, H., Nabavi-Pelesaraei, A., 2023. Illuminating sustainability: a comprehensive review of the environmental life cycle and exergetic impacts of solar systems on the agri-food sector. Sol. Energy 262, 111830. https://doi.org/10.1016/j.solener.2023.111830.

Hosokawa, M.N., Darros, A.B., Moris, V.A.d.S., Paiva, J.M.F.d., 2016. Polyhydroxybutyrate composites with random mats of sisal and coconut fibers. Mater. Res. 20, 279-290. https://doi.org/10.1590/1980-5373-MR-2016-0254.

Hosseinzadeh-Bandbafha, H., Safarzadeh, D., Ahmadi, E., Nabavi-Pelesaraei, A., Hosseinzadeh-Bandbafha, E., 2017. Applying data envelopment analysis to evaluation of energy efficiency and decreasing of greenhouse gas emissions of fattening farms. Energy 120, 652-662. https://doi.org/10.1016/j.energy.2016.11.117.

Huang, X., Guo, J., Gong, Y., Li, S., Mu, S., Zhang, S., 2017. In-situ preparation of a shape stable phase change material. Renew. Energ. 108, 244-249. https://doi.org/10.1016/j.renene.2017.02.083.

Huang, Z., Luo, P., Jia, S., Zheng, H., Lyu, Z., 2022a. A sulfur-doped carbon-enhanced Na_3V_2 $(PO_4)_3$ nanocomposite for sodium-ion storage. J. Phys. Chem. Solids 167, 110746. https://doi.org/10.1016/j.jpcs.2022.110746.

Huang, Z., Luo, P., Wu, Q., Zheng, H., 2022b. Constructing one-dimensional mesoporous carbon nanofibers loaded with $NaTi_2(PO_4)_3$ nanodots as novel anodes for sodium energy storage. J. Phys. Chem. Solids 161, 110479. https://doi.org/10.1016/j.jpcs.2021.110479.

Jiang, M., Wang, X., Xi, W., Zhou, H., Yang, P., Yao, J., Jiang, X., Wu, D., 2023. Upcycling plastic waste to carbon materials for electrochemical energy storage and conversion. Chem. Eng. J. 461, 141962. https://doi.org/10.1016/j.cej.2023.141962.

Keerthika, B., Umayavalli, M., Jeyalalitha, T., Krishnaveni, N., 2016. Coconut shell powder as cost effective filler in copolymer of acrylonitrile and butadiene rubber. Ecotoxicol. Environ. Saf. 130, 1-3. https://doi.org/10.1016/j.ecoenv.2016.03.022.

Kuang, W., Wang, H., Li, X., Zhang, J., Zhou, Q., Zhao, Y., 2018. Application of the thermodynamic extremal principle to diffusion-controlled phase transformations in Fe-CX alloys: Modeling and applications. Acta Mater. 159, 16-30. https://doi.org/10.1016/j.actamat.2018.08.008.

Lee, J.J.C., Hayat, N.N.A., Soo, X.Y.D., Tan, S.Y., Hnin, Y.Y.K., Wang, S., Wei, F., Kai, D., Wang, F., Luo, P., Xu, J., Loh, X.J., Zhu, Q., 2023. Upcycling of PET plastics into diethyl terephthalate for applications as phase change materials in energy harvesting. J. Energy Storage 73, 109084. https://doi.org/10.1016/j.est.2023.109084.

Lee, J.J.C., Sugiarto, S., Ong, P.J., Soo, X.Y.D., Ni, X., Luo, P., Hnin, Y.Y.K., See, J.S.Y., Wei, F., Zheng, R., Wang, P., Xu, J., Loh, X.J., Kai, D., Zhu, Q., 2022. Lignin-g-polycaprolactone as a form-stable phase change material for thermal energy storage application. J. Energy Storage 56, 106118. https://doi.org/10.1016/j.est.2022.106118.

Li, B., Shu, D., Wang, R., Zhai, L., Chai, Y., Lan, Y., Cao, H., Zou, C., 2020. Polyethylene glycol/silica (PEG@ SiO_2) composite inspired by the synthesis of mesoporous materials as shape-stabilized phase change material for energy storage. Renew. Energ. 145, 84-92. https://doi.org/10.1016/j.renene.2019.05.118.

Li, J., Luo, M., Zhao, C.-J., Li, C.-Y., Wang, W., Zu, Y.-G., Fu, Y.-J., 2013. Oil removal from water with yellow horn shell residues treated by ionic liquid. Bioresour. Technol. 128, 673-678. https://doi.org/10.1016/j.biortech.2012.11.009.

Li, M., Wang, C., 2019. Preparation and characterization of GO/PEG photo-thermal conversion form-stable composite phase change materials. Renew. Energ. 141, 1005-1012. https://doi.org/10.1016/j.renene.2019.03.141.

Liang, R., Yuan, H., Xi, G., Zhou, Q., 2009. Synthesis of wheat straw-g-poly (acrylic acid) superabsorbent composites and release of urea from it. Carbohydr. Polym. 77 (2), 181-187. https://doi.org/10.1016/j.carbpol.2008.12.018.

Liao, Y., Li, J., Li, S., Yang, X., 2022. Super-elastic and shape-stable solid-solid phase change materials for thermal management of electronics. J. Energy Storage 52, 104751. https://doi.org/10.1016/j.est.2022.104751.

Liu, Z., He, F., Li, Y., Jiang, Z., He, G., Lin, C., Zhang, Q., Zhou, Y., Yang, W., 2023. Enhanced solar/electric-to-thermal energy conversion capability of double skeleton based shape-stabilized phase change materials. Sol. Energy Mater. Sol. Cells 252, 112171. https://doi.org/10.1016/j.solmat.2022.112171.

Liu, Z., Tang, B., Zhang, S., 2020. Novel network structural PEG/PAA/SiO_2 composite phase change materials with strong shape stability for storing thermal energy. Sol. Energy Mater. Sol. Cells 216, 110678. https://doi.org/10.1016/j.solmat.2020.110678.

Lu, Y., Xiao, X., Fu, J., Huan, C., Qi, S., Zhan, Y., Zhu, Y., Xu, G., 2019. Novel smart textile with phase change materials encapsulated core-sheath structure fabricated by coaxial electrospinning. Chem. Eng. J. 355, 532-539. https://doi.org/10.1016/j.cej.2018.08.189.

Matei, C., Buhălţeanu, L., Berger, D., Mitran, R.-A., 2019. Functionalized mesoporous silica as matrix for shape-stabilized phase change materials. Int. J. Heat Mass Transfer 144, 118699. https://doi.org/10.1016/j.ijheatmasstransfer.2019.118699.

Mitran, R.-A., Lincu, D., Buhălţeanu, L., Berger, D., Matei, C., 2020. Shape-stabilized phase change materials using molten $NaNO_3$–KNO_3 eutectic and mesoporous silica matrices. Sol. Energy Mater. Sol. Cells 215, 110644. https://doi.org/10.1016/j.solmat.2020.110644.

Mittal, M., Chaudhary, R., 2019. Experimental investigation on the thermal behavior of untreated and alkali-treated pineapple leaf and coconut husk fibers. Int. J. Appl. Sci. Eng. 7 (1), 1-16. https://doi.org/10.30954/2322-0465.1.2019.1.

Muiruri, J.K., Yeo, J.C.C., Soo, X.Y.D., Wang, S., Liu, H., Kong, J., Cao, J., Tan, B.H., Suwardi, A., Li, Z., Xu, J., Loh, X.J., Zhu, Q., 2023. Recent Advances of Sustainable Short-chain length Polyhydroxyalkanoates (Scl-PHAs)–Plant Biomass Composites. Eur. Polym. J., 111882. https://doi.org/10.1016/j.eurpolymj.2023.111882.

Nabavi-Pelesaraei, A., Ghasemi-Mobtaker, H., Salehi, M., Rafiee, S., Chau, K.-W., Ebrahimi, R., 2023. Machine Learning Models of Exergoenvironmental Damages and Emissions Social Cost for Mushroom Production. Agronomy 13 (3), 737. https://doi.org/10.3390/agronomy13030737.

Nabavi-Pelesaraei, A., Saber, Z., Mostashari-Rad, F., Ghasemi-Mobtaker, H., Chau, K.-w., 2021. Coupled life cycle assessment and data envelopment analysis to optimize energy consumption and mitigate environmental impacts in agricultural production, in: Ren, J. (Ed.), Methods in Sustainability Science. Elsevier Inc, pp. 227-264.

Nguyen, G.T., Ly, T.N., Tran, N.T., Tuan, H.N.A., Hieu, N.H., Bui, T.H., 2023. Glutaric acid/expanded graphite composites as highly efficient shape-stabilized phase change materials at medium-temperature. J. Energy Storage 63, 107038. https://doi.org/10.1016/j.est.2023.107038.

Ong, P.J., Leow, Y., Soo, X.Y.D., Chua, M.H., Ni, X., Suwardi, A., Tan, C.K.I., Zheng, R., Wei, F., Xu, J., Loh, X.J., Kai, D., Zhu, Q., 2023a. Valorization of Spent coffee Grounds: A sustainable resource for Bio-based phase change materials for thermal energy storage. Waste Manage. (Oxford) 157, 339-347. https://doi.org/10.1016/j.wasman.2022.12.039.

Ong, P.J., Lum, Y.Y., Soo, X.Y.D., Wang, S., Wang, P., Chi, D., Liu, H., Kai, D., Lee, C.-L.K., Yan, Q., Xu, J., Loh, X.J., Zhu, Q., 2023b. Integration of phase change material and thermal insulation material as a passive strategy for building cooling in the tropics. Constr. Build. Mater. 386, 131583. https://doi.org/10.1016/j.conbuildmat.2023.131583.

Panepinto, D., Genon, G., 2012. Biomass thermal treatment: energy recovery, environmental compatibility and determination of external costs. Waste Biomass Valor. 3, 197-206. https://doi.org/10.1007/s12649-011-9099-x.

Phat, L.N., Nguyen, H.C., Khoa, B.D.D., Khang, P.T., Tien, D.X., Thang, T.Q., Trung, N.K., Nam, H.M., Phong, M.T., Hieu, N.H., 2022. Synthesis and surface modification of cellulose cryogels from coconut peat for oil adsorption. Cellulose 29 (4), 2435-2447. https://doi.org/10.1007/s10570-022-04427-7.

Png, Z.M., Soo, X.Y.D., Chua, M.H., Ong, P.J., Xu, J., Zhu, Q., 2022. Triazine derivatives as organic phase change materials with inherently low flammability. J. Mater. Chem. A 10 (7), 3633-3641. https://doi.org/10.1039/D1TA07422A

Pourebrahimi, S., 2022. Upcycling face mask wastes generated during COVID-19 into value-added engineering materials: A review. Sci. Total Environ. 851, 158396. https://doi.org/10.1016/j.scitotenv.2022.158396.

Qi, X., Yu, F., Meng, Z., Sun, Z., Zhang, N., Guo, Z., 2023. Preliminary design of the suppressive containment system based on HPR1000. Nucl. Eng. Des. 415, 112743. https://doi.org/10.1016/j.nucengdes.2023.112743.

Rathore, P.K.S., kumar Shukla, S., 2021. Improvement in thermal properties of PCM/Expanded vermiculite/expanded graphite shape stabilized composite PCM for building energy applications. Renew. Energ. 176, 295-304. https://doi.org/10.1016/j.renene.2021.05.068.

Ren, M., Zhao, H., Gao, X., 2022. Effect of modified diatomite based shape-stabilized phase change materials on multiphysics characteristics of thermal storage mortar. Energy 241, 122823. https://doi.org/10.1016/j.energy.2021.122823.

Saeed, T., Alam, M.K., Miah, M.J., Majed, N., 2021. Removal of heavy metals in subsurface flow constructed wetlands: Application of effluent recirculation. Environ. Sustain. Indic. 12, 100146. https://doi.org/10.1016/j.indic.2021.100146.

Saman, N., Johari, K., Song, S.-T., Kong, H., Cheu, S.-C., Mat, H., 2016. High removal efficiency of Hg (II) and MeHg (II) from aqueous solution by coconut pith—Equilibrium, kinetic and mechanism analyses. J. Environ. Chem. Eng. 4 (2), 2487-2499. https://doi.org/10.1016/j.jece.2016.04.033.

Sireesha, S., Sreedhar, I., 2023. Holistic and parametric optimization study on Cr (VI) removal using acid-treated coco peat biochar adsorbent. Bioresource Technology Reports, 101486. https://doi.org/10.1016/j.biteb.2023.101486.

Soo, X.Y., Muiruri, J.K., Yeo, J.C., Png, Z.M., Sng, A., Xie, H., Ji, R., Wang, S., Liu, H., Xu, J., Loh, X.J., Yan, Q., Li, Z., Zhu, Q., 2023. Polyethylene glycol/polylactic acid block co-polymers as solid–solid phase change materials. SmartMat, e1188. https://doi.org/10.1002/smm2.1188.

Soo, X.Y.D., Png, Z.M., Wang, X., Chua, M.H., Ong, P.J., Wang, S., Li, Z., Chi, D., Xu, J., Loh, X.J., Zhu, Q., 2022. Rapid UV-curable form-stable polyethylene-glycol-based phase change material. ACS Appl. Polym. Mater. 4 (4), 2747-2756. https://doi.org/10.1021/acsapm.2c00059.

Sun, K., Kou, Y., Zheng, H., Liu, X., Tan, Z., Shi, Q., 2018. Using silicagel industrial wastes to synthesize polyethylene glycol/silica-hydroxyl form-stable phase change materials for thermal energy storage applications. Sol. Energy Mater. Sol. Cells 178, 139-145. https://doi.org/10.1016/j.solmat.2018.01.016.

Tang, T., Kyaw, A.K.K., Zhu, Q., Xu, J., 2020. Water-dispersible conducting polyazulene and its application in thermoelectrics. Chem. Commun. 56 (65), 9388-9391. https://doi.org/10.1039/D0CC03840G.

Thakur, K., Kalia, S., Kaith, B., Pathania, D., Kumar, A., 2015. Surface functionalization of coconut fibers by enzymatic biografting of syringaldehyde for the development of biocomposites. RSC Adv. 5 (94), 76844-76851. https://doi.org/10.1039/C5RA14891J.

Verasoundarapandian, G., Zakaria, N.N., Shaharuddin, N.A., Khalil, K.A., Puasa, N.A., Azmi, A.A., Gomez-Fuentes, C., Zulkharnain, A., Wong, C.Y., Rahman, M.F., 2021. Coco peat as agricultural waste sorbent for sustainable diesel-filter system. Plants 10 (11), 2468. https://doi.org/10.3390/plants10112468.

Wang, J., Zheng, Y., Wang, A., 2013. Investigation of acetylated kapok fibers on the sorption of oil in water. J. Environ. Sci. 25 (2), 246-253. https://doi.org/10.1016/S1001-0742(12)60031-X.

Wang, K., Zhu, J., Wang, H., Yang, K., Zhu, Y., Qing, Y., Ma, Z., Gao, L., Liu, Y., Wei, S., Shu, Y., Zhou, Y., He, J., 2022. Air plasma-sprayed high-entropy $(Y_{0.2}Yb_{0.2}Lu_{0.2}Eu_{0.2}Er_{0.2})_3Al_5O_{12}$ coating with high thermal protection performance. J. Adv. Ceram. 11 (10), 1571-1582. https://doi.org/10.1007/s40145-022-0630-2.

White, J.E., Catallo, W.J., Legendre, B.L., 2011. Biomass pyrolysis kinetics: a comparative critical review with relevant agricultural residue case studies. J. Anal. Appl. Pyrolysis 91 (1), 1-33. https://doi.org/10.1016/j.jaap.2011.01.004.

Wu, B., Jiang, Y., Wang, Y., Zhou, C., Zhang, X., Lei, J., 2018. Study on a PEG/epoxy shape-stabilized phase change material: preparation, thermal properties and thermal storage performance. Int. J. Heat Mass Transfer 126, 1134-1142. https://doi.org/10.1016/j.ijheatmasstransfer.2018.05.153.

Wu, B., Lyu, S., Han, H., Li, T., Sun, H., Wang, J.-K., Li, D., Lei, F., Huang, J., Sun, D., 2021. Biomass-based shape-stabilized phase change materials from artificially cultured ship-shaped diatom frustules with high enthalpy for thermal energy storage. Compos. B. Eng. 205, 108500. https://doi.org/10.1016/j.compositesb.2020.108500.

Wu, W.Y., Yeo, G.M.D., Wang, S., Liu, Z., Loh, X.J., Zhu, Q., 2023. Recent Progress in Polyethylene-enhanced Organic Phase Change Composite Materials for Energy Management. Chem. Asian J. 18 (14), e202300391. https://doi.org/10.1002/asia.202300391.

Xin, T., Tang, S., Ji, F., Cui, L., He, B., Lin, X., Tian, X., Hou, H., Zhao, Y., Ferry, M., 2022. Phase transformations in an ultralight BCC Mg alloy during anisothermal ageing. Acta Mater. 239, 118248. https://doi.org/10.1016/j.actamat.2022.118248.

Xiong, W., Chen, Y., Hao, M., Zhang, L., Mei, T., Wang, J., Li, J., Wang, X., 2015. Facile synthesis of PEG based shape-stabilized phase change materials and their photo-thermal energy conversion. Appl. Therm. Eng. 91, 630-637. https://doi.org/10.1016/j.applthermaleng.2015.08.063.

Yan, D., Ming, W., Liu, S., Yin, G., Zhang, Y., Tang, B., Zhang, S., 2021. Polyethylene glycol (PEG)/silicon dioxide grafted aminopropyl group and carboxylic multi-walled carbon nanotubes (SAM) composite as phase change material for light-to-heat energy conversion and storage. J. Energy Storage 36, 102428. https://doi.org/10.1016/j.est.2021.102428.

Yang, G., Zhao, L., Shen, C., Mao, Z., Xu, H., Feng, X., Wang, B., Sui, X., 2020. Boron nitride microsheets bridged with reduced graphene oxide as scaffolds for multifunctional shape stabilized phase change materials. Sol. Energy Mater. Sol. Cells 209, 110441. https://doi.org/10.1016/j.solmat.2020.110441.

Yang, L., Wang, Z., Yang, L., Li, X., Zhang, Y., Lu, C., 2017. Coco peat powder as a source of magnetic sorbent for selective oil–water separation. Ind. Crops Prod. 101, 1-10. https://doi.org/10.1016/j.indcrop.2017.02.040.

Yang, R., Zheng, N., Yu, Z., Zhang, F., Gai, H., Chen, J., Huang, X., 2023. Nickel foam/Covalent-Organic Frameworks for composite phase change materials with enhanced solar-thermal energy conversion and storage capacity. Appl. Therm. Eng. 230, 120808. https://doi.org/10.1016/j.applthermaleng.2023.120808.

Yang, S., Huang, Z., Hu, Q., Zhang, Y., Wang, F., Wang, H., Shu, Y., 2022a. Proportional optimization model of multiscale spherical BN for enhancing thermal conductivity. ACS Appl. Electron. Mater. 4 (9), 4659-4667. https://doi.org/10.1021/acsaelm.2c00878.

Yang, S., Zhang, Y., Sha, Z., Huang, Z., Wang, H., Wang, F., Li, J., 2022b. Deterministic Manipulation of Heat Flow via Three-Dimensional-Printed Thermal Meta-Materials for Multiple Protection of Critical Components. ACS Appl. Mater. Interfaces 14 (34), 39354-39363. https://doi.org/10.1021/acsami.2c09602.

Yang, Y., Yin, Q., Xu, F., Sun, L., Xia, Y., Guan, Y., Liao, L., Zhou, T., Lao, J., Wang, Y., 2022c. Fabricated Polyethylene glycol/hydroxylated carbon nanotubes shape-stabilized phase change materials with improving thermal conductivity. Thermochim. Acta 718, 179363. https://doi.org/10.1016/j.tca.2022.179363.

Yin, G.-Z., Palencia, J.L.D., Wang, D.-Y., 2021. Fully bio-based Poly (Glycerol-Itaconic acid) as supporter for PEG based form stable phase change materials. Compos. Commun. 27, 100893. https://doi.org/10.1016/j.coco.2021.100893.

Yong, X., Wu, G., Shi, W., Wong, Z.M., Deng, T., Zhu, Q., Yang, X., Wang, J.-S., Xu, J., Yang, S.-W., 2020. Theoretical search for high-performance thermoelectric donor–acceptor copolymers: the role of super-exchange couplings. J. Mater. Chem. A 8 (41), 21852-21861. https://doi.org/10.1039/D0TA05765G.

Zare, P., Perera, N., Lahr, J., Hasan, R., 2022. Solid-liquid phase change materials for the battery thermal management systems in electric vehicles and hybrid electric vehicles–A systematic review. J. Energy Storage 52, 105026. https://doi.org/10.1016/j.est.2022.105026.

Zhang, L., Wang, Y., Ding, B., Gu, J., Ukrainczyk, N., Cai, J., 2023a. Development of geopolymer-based composites for geothermal energy applications. J. Clean. Prod. 419, 138202. https://doi.org/10.1016/j.jclepro.2023.138202.

Zhang, Q., Xue, T., Tian, J., Yang, Y., Fan, W., Liu, T., 2022. Polyimide/boron nitride composite aerogel fiber-based phase-changeable textile for intelligent personal thermoregulation. Compos. Sci. Technol. 226, 109541. https://doi.org/10.1016/j.compscitech.2022.109541.

Zhang, X., Yin, Z., Meng, D., Huang, Z., Wen, R., Huang, Y., Min, X., Liu, Y., Fang, M., Wu, X., 2017. Shape-stabilized composite phase change materials with high thermal conductivity based on stearic acid and modified expanded vermiculite. Renew. Energ. 112, 113-123. https://doi.org/10.1016/j.renene.2017.05.026.

Zhang, Y., He, X., Cong, X., Wang, Q., Yi, H., Li, S., Zhang, C., Zhang, T., Wang, X., Chi, Q., 2023b. Enhanced energy storage performance of polyethersulfone-based dielectric composite via regulating

heat treatment and filling phase. J. Alloys Compd. 960, 170539. https://doi.org/10.1016/j.jallcom.2023.170539.

Zhao, Y., Zhang, B., Hou, H., Chen, W., Wang, M., 2019. Phase-field simulation for the evolution of solid/liquid interface front in directional solidification process. J. Mater. Sci. Technol. 35 (6), 1044-1052. https://doi.org/10.1016/j.jmst.2018.12.009.

Zhou, X., He, P., Peng, W., Lü, F., Shao, L., Zhang, H., 2023. Upcycling of real-world HDPE plastic wastes into high-purity methane and hierarchical porous carbon materials: influence of plastics additives. J. Environ. Chem. Eng. 11 (2), 109327. https://doi.org/10.1016/j.jece.2023.109327.

Zhu, H., Lu, Y., Cai, L., 2023a. Wavelength-shift-free racetrack resonator hybrided with phase change material for photonic in-memory computing. Opt. Express 31 (12), 18840-18850. https://doi.org/10.1364/OE.489525.

Zhu, Q., Ong, P.J., Goh, S.H.A., Yeo, R.J., Wang, S., Liu, Z., Loh, X.J., 2023b. Recent advances in graphene-based phase change composites for thermal energy storage and management. Nano Mater. Sci. https://doi.org/10.1016/j.nanoms.2023.09.003.

Zhu, Q., Yildirim, E., Wang, X., Kyaw, A.K.K., Tang, T., Soo, X.Y.D., Wong, Z.M., Wu, G., Yang, S.-W., Xu, J., 2020. Effect of substituents in sulfoxides on the enhancement of thermoelectric properties of PEDOT: PSS: experimental and modelling evidence. Mol. Syst. Des. Eng. 5 (5), 976-984. https://doi.org/10.1039/D0ME00032A.